Enhancement of optical absorption in thin-film organic solar cells through the excitation of plasmonic modes in metallic gratings

Changjun Min,[1] Jennifer Li,[1] Georgios Veronis,[1,2,a)] Jung-Yong Lee,[3] Shanhui Fan,[3] and Peter Peumans[3]
[1]*Center for Computation and Technology, Louisiana State University, Baton Rouge, Louisiana 70803, USA*
[2]*Department of Electrical and Computer Engineering, Louisiana State University, Baton Rouge, Louisiana 70803, USA*
[3]*Department of Electrical Engineering, Stanford University, Stanford, California 94305, USA*

(Received 15 December 2009; accepted 7 March 2010; published online 30 March 2010)

We theoretically investigate the enhancement of optical absorption in thin-film organic solar cells in which the top transparent electrode is partially substituted by a periodic metallic grating. We show that the grating can result in broadband optical absorption enhancement for TM-polarized light, due to the large field enhancement in the vicinity of the strips of the grating, associated with the excitation of plasmonic modes. The overall optical absorption in the organic layers can be greatly enhanced up to ~50% for such solar cell structures. © *2010 American Institute of Physics*. [doi:10.1063/1.3377791]

Thin-film organic solar cells (OSCs) are a promising candidate for low-cost energy conversion.[1–6] However, significant improvement in the efficiency of the cells is required to make them competitive with grid power.[7] In thin-film OSCs, the active layer thickness must be smaller than the excitonic diffusion length.[4] This, however, limits the photon absorption efficiency. Recently, it has been demonstrated that the use of metallic nanostructures in solar cells results in optical field enhancement, and improvement of the optical absorption.[5,8–12]

In this letter, we theoretically investigate the effect of introducing metallic gratings in thin-film OSCs on their optical absorption efficiency. More specifically, we consider OSCs in which the top transparent electrode is partially substituted by a periodic silver grating. We find that, for TM-polarized light, the metallic strips of the grating can result in broadband optical absorption enhancement with respect to solar cells without grating. This is due to the large field enhancement in the vicinity of the metallic grating, associated with the excitation of plasmonic modes. For TE-polarized light, the metallic grating results in slight suppression in optical absorption. However, the absorption enhancement for TM light is much larger than the absorption suppression for TE light, so that the overall optical absorption is greatly enhanced up to ~50% under AM1.5 illumination.

A schematic of the OSCs investigated is shown in Fig. 1(a). The top transparent PEDOT electrode typically used in conventional OSCs is partially substituted by a periodic silver grating in order to excite plasmonic modes. The active layers of such solar cell structure, a 4 nm thick electron acceptor layer (PTCBI) and an 11 nm thick donor layer (CuPc), are chosen thin to ensure large exciton collection.[4] The BCP layer functions as a transparent spacer layer that transports electrons to the bottom optically-thick Ag electrode.[1] We use a full-wave finite-difference frequency-domain electromagnetic simulation method[13] to calculate the optical absorption in such structures. This method allows us to directly use experimental data for the frequency-dependent dielectric constant of materials such as silver,[14] including both the real and imaginary parts, with no approximation. The frequency-dependent dielectric constants of organic materials (CuPc and PTCBI) were obtained from spectroscopic ellipsometry measurements.[4] Plane waves are incident on the structure. Periodic boundary conditions[15] are used at the left and right boundaries, while perfectly matched layer absorbing boundary conditions[16] are used at the top and bottom boundaries of the simulation domain.

We consider the effect of the metallic grating on optical absorption in such structures. In Fig. 1(b), we show the absorption spectra in the organic layers (CuPc and PTCBI) and

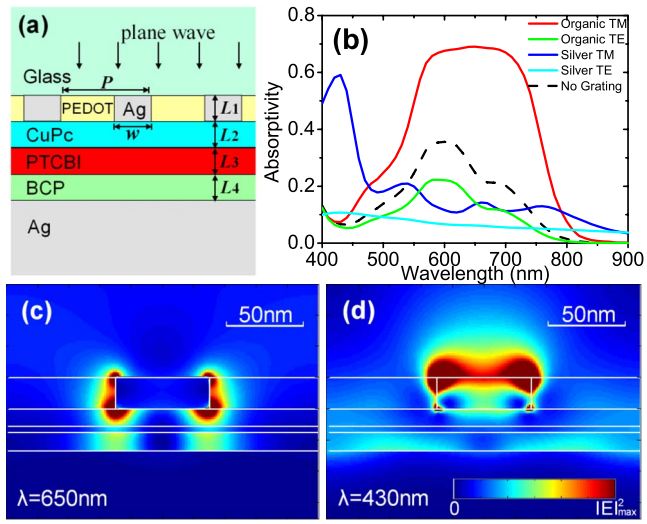

FIG. 1. (Color online) (a) Schematic of a thin-film OSC in which the top transparent PEDOT electrode is partially substituted by a periodic silver grating. (b) Absorption spectra in the organic layers (CuPc and PTCBI) of the solar cell for normally-incident TM-(TE-) polarized light. We also show the absorption spectra in the silver grating for TM-(TE-) polarized light, and the absorption spectra in the organic layers of a solar cell without grating. Results are shown for $P=200$ nm, $w=60$ nm, $L_1=20$ nm, $L_2=11$ nm, $L_3=4$ nm, and $L_4=12$ nm. [(c)–(d)] Electric field intensity profile for a solar cell structure with metallic grating for normally-incident TM-polarized light at $\lambda=650$ and 430 nm. One period of the structure is shown. All other parameters are as in (b).

a)Electronic mail: gveronis@lsu.edu.

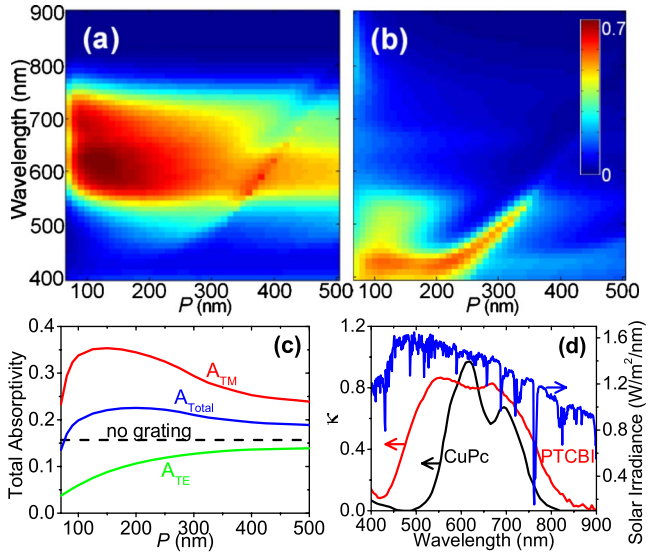

FIG. 2. (Color online) [(a)–(b)] Absorption in the organic material layers, and the metallic grating for normally-incident TM-polarized light as a function of grating periodicity P and wavelength. Results are shown for w=50 nm. All other parameters are as in Fig. 1(b). (c) Total TM (TE) absorptivity A_{TM} (A_{TE}) as a function of grating periodicity P for normally-incident light. We also show the overall absorptivity A_{Total} of the solar cell, as well as A_{Total} of a cell without grating. All parameters are as in (a). (d) Imaginary part κ of the refractive index as a function of wavelength for the organic materials CuPc and PTCBI. We also show the solar irradiance spectrum.

in the metallic grating for normally-incident TM- and TE-polarized light. For TM-polarized light, the absorption spectrum in organic layers shows broadband enhancement compared to the spectrum of a solar cell without grating in the wavelength range $450\ \text{nm} \leq \lambda \leq 850$ nm. Examining the field pattern at the peak of this absorption band (λ =650 nm), we notice strong field enhancement especially throughout the CuPc organic layer [Fig. 1(c)]. This is due to a broadband surface plasmon mode that is concentrated in the silver-organic layer interface (SO-SP mode). In contrast, the absorption spectrum in the silver region exhibits a sharp peak at λ=430 nm. Examining the field pattern at this peak [Fig. 1(d)], we note that it is associated with a surface plasmon mode that is concentrated in the silver-glass interface (SG-SP mode). Thus, the asymmetry in the structure, in the form of index difference between the CuPc organic layer ($n \sim 1.8$) and glass ($n \sim 1.5$) enables us to spectrally separate out the absorption in the silver region, which is undesirable, from the beneficial absorption enhancement in the organic layers. As a result, the solar cell parameters can be tuned, so that the SO-SP mode wavelength range and the SG-SP mode wavelength range have maximum and minimum overlap, respectively, with the high-absorption range of organic materials. In contrast, for TE-polarized light, the metallic grating results in slight suppression of the absorption in organic layers [Fig. 1(b)], since the grating blocks part of the incident light, and the very thin organic layers here do not support any TE waveguide modes, which are known to enhance the absorption in thicker film solar cell structures.[8,11] The TE absorption in the silver grating is lower than the TM absorption, since no plasmonic TE modes are excited.

We next consider the effect of grating periodicity P on the optical absorption. In Figs. 2(a) and 2(b), we show the absorption in the organic layers and the metallic grating, respectively, for normally-incident TM-polarized light, as a function of grating periodicity P and wavelength. We observe broadband high absorption for $80\ \text{nm} < P < 300$ nm, associated with the SO-SP mode [Fig. 2(a)]. Strong absorption is observed for a wide range of grating periodicities P, because the properties of the SO-SP mode supported by the periodic metallic strips are mainly determined by the strip width w and thickness L_1, and are weakly dependent on P for $P > 100$ nm. For periodicities $P < 100$ nm, we found that the field of the SO-SP mode is concentrated in the slits between strips, hence the absorption in the organic layers decreases. The SG-SP mode results in high absorption in the silver strips for $200\ \text{nm} < P < 350$ nm [Fig. 2(b)]. Such absorption is narrowband, because the SG-SP mode is excited only when the grating phase-matching condition is satisfied.[17] We also observe that the SG-SP mode causes narrowband absorption in the organic layers for $350\ \text{nm} < P < 450$ nm[Fig. 2(a)], which has therefore little contribution to the overall absorption in organic layers.

We define the *total absorptivity* over all wavelengths for TM- and TE-polarized light as

$$A_{TM} \equiv \frac{\int_0^\infty a_{TM}(\lambda) S(\lambda) d\lambda}{\int_0^\infty S(\lambda) d\lambda}, \quad A_{TE} \equiv \frac{\int_0^\infty a_{TE}(\lambda) S(\lambda) d\lambda}{\int_0^\infty S(\lambda) d\lambda},$$

where $a_{TM}(\lambda)$ [$a_{TE}(\lambda)$] is the absorption spectrum in organic layers for TM-(TE-) polarized light, and $S(\lambda)$ is the solar irradiance spectrum [Fig. 2(d)]. In Fig. 2(c), we show the total absorptivities A_{TM} and A_{TE} as a function of grating periodicity P for normally-incident light, compared to the case of solar cells without grating. We observe a broad peak in A_{TM} due to the large field enhancement from the SO-SP mode. For $P \leq 100$ nm A_{TM} decreases due to the concentration of the SO-SP modal field in the PEDOT slits, as mentioned above. A_{TM} also decreases with P for $P > 200$ nm, since the effect of plasmonic absorption enhancement in the vicinity of the strips becomes weaker as P increases. On the other hand, when P increases, more TE light can transmit through the slits of the grating, and A_{TE} therefore increases. Since the absorption enhancement in the TM case is much larger than the absorption suppression in the TE case, the overall absorption $A_{Total} = (A_{TM} + A_{TE})/2$ is greatly enhanced for a large range of P.

We now consider the effect of strip width w and thickness L_1 on the absorption in the organic layers. In Figs. 3(a) and 3(b), we show A_{TM}, A_{TE}, and A_{Total} as a function of w and L_1, respectively, for normally-incident light, compared to solar cells without grating. As mentioned above, the properties of the SO-SP mode are mostly determined by the strip width w and thickness L_1. When w and L_1 are chosen so that the SO-SP mode wavelength range optimally overlaps with the high-absorption wavelength range of organic materials [Fig. 2(d)], a TM absorption peak is observed [Figs. 3(a) and 3(b)]. For TE-polarized light, larger metallic width w blocks more incident light, and increased metallic thickness L_1 allows less light to transmit through the slits of the grating, so that A_{TE} decreases with both w and L_1. However, the overall absorption A_{Total} is enhanced for a large range of w and L_1, due to the much stronger enhancement in A_{TM}.

In Fig. 3(c), we show the *total absorption enhancement*, defined as the ratio of A_{Total} with grating to A_{Total} without grating, as a function of the periodicity P and the strip width w for normally-incident light. We observe that, for increasing

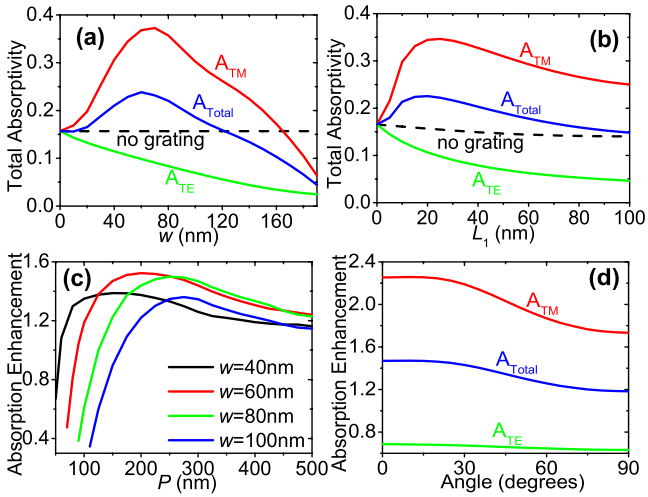

FIG. 3. (Color online) (a) Total TM (TE) absorptivity A_{TM} (A_{TE}) as a function of grating width w for normally-incident light. We also show the overall absorptivity A_{Total} of the solar cell, as well as A_{Total} of a cell without grating. All other parameters are as in Fig. 1(b). (b) A_{TM} (A_{TE}) as a function of grating thickness L_1 for normally-incident light. We also show A_{Total} of the solar cell, as well as A_{Total} of a cell without grating. Results are shown for w=50 nm. All other parameters are as in Fig. 1(b). Note that A_{Total} of the solar cell without grating slightly decreases with L_1, due to the weak absorption in PEDOT layer. (c) Total absorption enhancement as a function of grating periodicity P for w=40, 60, 80, and 100 nm. All other parameters are as in Fig. 1(b). (d) Total TM (TE) absorption enhancement as a function of incident angle. We also show the total absorption enhancement of the solar cell. Results are shown for w=50 nm. All other parameters are as in Fig. 1(b).

w, the enhancement peak shifts to larger P. This is due to the fact that the width P-w of the slits between neighboring metallic strips has to be large enough to avoid concentration of the SO-SP modal field in the slits. The maximum enhancement of ~50% is obtained for w=60 nm, due to the optimal overlap between the SO-SP mode wavelength range and the high-absorption wavelength range of organic materials. We also found similar enhancements for devices with indium tin oxide top electrodes.

Finally, in Fig. 3(d) we show the effect of incident angle on the total absorption enhancement. Even though the optical absorption in the organic layers decreases rapidly at large angles due to the large reflection at the air/glass interface, the absorption enhancement is weakly dependent on the angle of incidence. This is due to the fact that the SO-SP mode is broadband [Fig. 2(a)], and is excited for a wide range of angles of incidence.

G.V. acknowledges the support of the Louisiana Board of Regents (Contract No. LEQSF(2009-12)-RD-A-08). S.F. acknowledges the support of the Center for Advanced Molecular Photovoltaics (CAMP) (Award No KUSC1-015-21), made by King Abdullah University of Science and Technology, and of DOE under Grant No. DE-FG02-07ER46426.

[1] P. Peumans and S. R. Forrest, Appl. Phys. Lett. **79**, 126 (2001).
[2] G. Li, V. Shrotriya, J. Huang, Y. Yao, T. Moriarty, K. Emery, and Y. Yang, Nature Mater. **4**, 864 (2005).
[3] J. Y. Kim, K. Lee, N. E. Coates, D. Moses, T.-Q. Nguyen, M. Dante, and A. J. Heeger, Science **317**, 222 (2007).
[4] M. Agrawal and P. Peumans, Opt. Express **16**, 5385 (2008).
[5] N. C. Lindquist, W. A. Luhman, S. H. Oh, and R. J. Holmes, Appl. Phys. Lett. **93**, 123308 (2008).
[6] D. H. Ko, J. R. Tumbleston, L. Zhang, S. Williams, J. M. DeSimone, R. Lopez, and E. T. Samulski, Nano Lett. **9**, 2742 (2009).
[7] S. R. Forrest, Nature (London) **428**, 911 (2004).
[8] N. C. Panoiu and R. M. Osgood, Opt. Lett. **32**, 2825 (2007).
[9] K. R. Catchpole and A. Polman, Opt. Express **16**, 21793 (2008).
[10] V. E. Ferry, L. A. Sweatlock, D. Pacifici, and H. A. Atwater, Nano Lett. **8**, 4391 (2008).
[11] R. A. Pala, J. White, E. Barnard, J. Liu, and M. L. Brongersma, Adv. Mater. **21**, 3504 (2009).
[12] H. Shen, P. Bienstman, and B. Maes, J. Appl. Phys. **106**, 073109 (2009).
[13] G. Veronis and S. Fan, in *Surface Plasmon Nanophotonics*, edited by M. L. Brongersma and P. G. Kik (Springer, Berlin, Heidelberg, 2007).
[14] E. D. Palik, *Handbook of Optical Constants of Solids* (Academic, New York, 1985).
[15] S. Fan, P. R. Villeneuve, and J. D. Joannopoulos, Phys. Rev. B **54**, 11245 (1996).
[16] J. Jin, *The Finite Element Method in Electromagnetics* (Wiley, New York, 2002).
[17] S. A. Maier, *Plasmonics: Fundamentals and Applications* (Springer, New York, 2007).